Elastic property of multiphase composites with random microstructures

Moran Wang [*],[1], Ning Pan

Nanomaterials in the Environment, Agriculture and Technology (NEAT), University of California at Davis, CA 95616, USA

ABSTRACT

We propose a computational method with no *ad hoc* empirical parameters to determine the elastic properties of multiphase composites of complex geometries by numerically solving the stress–strain relationships in heterogeneous materials. First the random microstructure of the multiphase composites is reproduced in our model by the random generation-growth method. Then a high-efficiency lattice Boltzmann method is employed to solve the governing equation on the multiphase microstructures. After validated against a few standard solutions for simple geometries, the present method is used to predict the effective elastic properties of real multiphase composites. The comparisons between the predictions and the existing experimental data have shown that the effects of pores/voids in composites are not negligible despite their seemingly tiny amounts. Ignorance of such effects will lead to over-predictions of the effective elastic properties compared with the experimental measurements. When the pores are taken into account and treated as a separate phase, the predicted Young's modulus, shear modulus and Poisson's ratio agree well with the available experimental data. The present method provides an alternative tool for analysis, design and optimization of multiphase composite materials.

Published by Elsevier Inc.

1. Introduction

The problem of determining the effective linear elastic properties of multiphase composites with complex microstructures is a classical, important and yet challenging issue, with applications in almost every area of material sciences [1–5]. The effective elastic modulus is one of the most important properties that characterize the mechanical performance of materials. As is well known now, the effective elastic modulus of a multiphase composite depends not only on the corresponding elastic properties and the volume fraction of each constitute component, but on the microstructures (i.e., the spatial distribution of the components) of the composite as well [4]. The theoretical approaches found in the literature for predicting the effective elastic modulus are mostly based on the effective medium theories which in essence provide approximate estimations of the effective modulus by homogenizing the complex medium [6]. Inevitably empirical parameters have been introduced into the models to account for the influence of the structural variations on the results [3,7]. Another alternative group of analytical approaches is to provide upper and lower bounds, which were rigorously derived theoretically and then validated through experimental data [1,8,9]. In terms of experimental techniques, there have been numbers of measurement schemes developed over the years. However more often than not, it is difficult to compare the theoretical predictions with the experimental data, for many important features and mechanisms in a complex material, such as the shapes and spatial distribution of inclusions, and connections and interaction between different phases, are difficult to be accounted for in a theoretical model, other than making a few rough assumptions to either ignore or over-simplify them. On the experimental

---

side, the current technology is still not advanced enough to detect many local, random and often irregular factors that collectively impact the material behaviors in a significant way.

Furthermore, the existing theories fall even short when coming to design non-existent novel materials, for instance the meta-materials, where initial design and optimization have to rely on theories [3].

Computer numerical simulation has provided a promising new way in this regard, owing to the rapid developments of computers and computational techniques in the past few decades. A useful numerical scheme in dealing with complex materials generally should include two major components: reproducing the microstructures of the materials so as to bring the inherent structural complicities and internal interactions into the computer as the first and critical step, and then solving the relevant set of governing equations on the given structure. In terms of generating computerized material structures, several methods have been proposed focusing on multiphase composites. The *random location of obstacles* proposed by Zhang et al. in 2006 [10] is the simplest one in constructing an artificial random microstructure, however, the approach is too primitive to catch some of the important structural details. Snyder et al. [3] proposed a more advanced method to generate randomly distributed circular inclusions on hexagonal pixels. Digital micro-tomographic information and statistical correlation functions have been adopted in reconstruction of the structures more accurately [9,11,12]. Inspired by the spirit of the cluster growing theory [13], Wang et al. [14] have recently developed a simpler method, the random generation-growth (RGG) method, to reproduce the random microstructures of multiphase porous media. The generated microstructure is conveniently controlled by a few statistical parameters each of which has a clear physical significance. The RGG method has shown success in predicting thermal conductivities of various multiphase media, as validated by the experimental data [14,15].

After the reconstruction of materials via the algorithms, the relevant governing equations have to be solved. However such traditional PDE solvers as the finite-difference scheme [4] or the popular finite-element technique [16,17] require vast grid refinements and thus demand huge computational resources when the geometries of the microstructure are complex, especially for multiphase conjugate cases. A high-efficiency lattice Boltzmann method (LBM) has recently been developed to tackle various PDEs with conservation and conjugation effects during evolution of thermal and electrical transport problems [18,19]. Since complex geometry boundary conditions can be easy implemented in LBM [20–24], application of this approach to solving the governing equations of elastic mechanics in multiphase composites becomes a logical development.

This contribution aims to develop a numerical method in calculating or predicting the effective elastic properties of multiphase composites. We first devise the random generation-growth method for reproducing the microstructures of three-phase (3 P) composites and then solve the governing equations by the LBM method. The calculated elastic moduli will be compared with existing experimental data and the physical mechanisms involved will be discussed.

2. The numerical scheme

This section will describe the details of the numerical model, its basic assumptions and the governing equations. The new approach reproduces the multiphase microstructure by the random generation-growth method and solves the governing equations by the LBM algorithm.

2.1. Basic hypothesis and equations

Consider a simple pure elastic compression test on a multiphase composite as shown in Fig. 1. The bottom surface of the domain is fixed and the top surface is under a uniform normal compressive force, F. We suppose only small elastic strain occurs in the direction of the force without any multi-dimensional effects. After reaching a steady state, the governing equation for describing the displacement field can be expressed by a simple Poisson equation [25], i.e.

$$\nabla \cdot \{E(r)\nabla[A(r)U(r)]\} = 0 \tag{1}$$

where E is the local Young's modulus, r the position, A the cross-sectional area, and U the displacement in the direction of force. Since no slippage is considered, Eq. (1) is subjected to the stress and strain continuities at each interface between two phases (i,j):

$$U|_{int,i} = U|_{int,j} \tag{2}$$

$$E_i \cdot \nabla U|_{int,i} = E_j \cdot \nabla U|_{int,j} \tag{3}$$

The force F on the top surface leads to a second-type (Neumann) boundary condition. However since the application of F, under the pure elastic assumption, does not alter the effective property noticeably, we use the Dirichlet boundary condition by assigning a known displacement, U_1, at the top surface and U_0 at the bottom:

$$U|_{top} = U_1 \tag{4}$$

$$U|_{bottom} = U_0 \tag{5}$$

While the periodic boundary conditions are implemented on the both sides. Once the displacement field is solved, the effective Young's modulus of the composite is obtained as
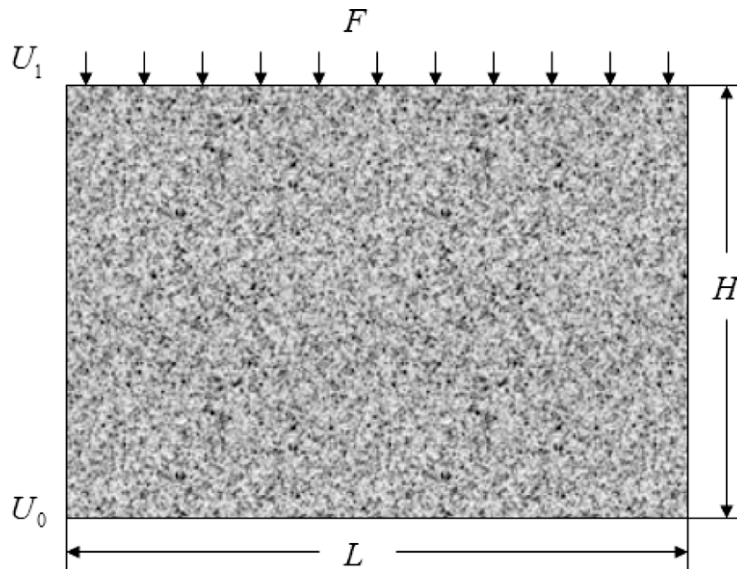
Fig. 1. Schematic diagram of stress and strain boundaries for a multiphase composite.

$$E_{eff} = \frac{stress}{strain} = \frac{F/A}{\Delta U/H} \tag{6}$$

where the external force F is calculated as

$$F = E \cdot A \nabla U \tag{7}$$

Eqs. (1)–(7) describe a simple yet novel way to determine the effective Young's modulus of a heterogeneous multiphase composites by solving a Poisson equation at given conditions. Although is the case shown here is one-dimensional, it could be extended to three-dimensional problems [26,27]. Another interesting thing is that if the external force on the top surface is a shear force, i.e. tractions on top and bottom surfaces, and the shear displacement U only occurs in the shear direction, i.e., simple shear, the current method can be extended to calculating the effective shear moduli of the system.

2.2. Structure reproduction

We have proposed a general random generation-growth algorithm in our previous work [14]. Here we adopt it for reproducing the microstructure of a composite of two solid components, one dispersed into the other continuous matrix, and containing small amount of voids (or air), thus actually a three-phase system [28,29]. Before the generation process, we select the continuous solid phase as the non-growing phase, the dispersed solid as the first growing phase and the voids (or pores) the second growing phase. We use a superscript number below to indicate the corresponding growing phase. The growing process is then conducted as follows.

(i) Randomly locate cores/seeds of the first growing phase in a grid system based on a core distribution probability, c_d^1, whose value is no greater than the volume fraction of the phase. Each cell in the grid will be assigned a random number of a uniform distribution function within $(0,1)$. Each cell whose random number is no greater than c_d^1 will be chosen as a core/seed;

(ii) Expand every element of the growing phase to its neighboring cells in each direction based on the given directional growth probability, D_i^1, where i represents the direction. Again for each growing element, new random numbers will be assigned to its neighboring cells. The neighboring cell in direction i will become part of the growing phase if its random number is no greater than D_i^1;

(iii) Repeat the growing process of (ii) until the volume fraction of the first growing phase reaches its given value ϕ^1;

(iv) As to the second growing phase (pores), we treat the pores as another discrete growing phase. Therefore it grows from separate seeds, very similar to the process for the first growing phase described in (i)–(iii), yet controlled by c_d^2 and D_i^2 correspondingly.

(v) Stop the pores growth once its volume fraction reaches the given value ϕ^2 (or more often expressed as the porosity ε).

Thus the generated microstructure of multiphase composites can be controlled by three parameters (c_d, D_i, ϕ) for each growing phase. Every parameter in the generation process has a physical significance and can be determined through experimental observation and measurements. The core distribution probability c_d is defined as the probability of a cell/grid to

become to a core of the growing phase and it value depends on the number density of the growing units. For a growing phase with a given volume fraction v_f, the value of c_d could be determined by

$$c_d = \phi \cdot V / (N \cdot \overline{V_p})$$

(8)

with V representing the total volume of the system, N the total grid number and $\overline{V_p}$ the average volume of the growing particles/pores.

The directional growth probability D_i is defined as the probability for a yet-to-be-occupied cell to merge into a neighboring cell in the ith direction so as to become part of the growing phase. An appropriate arrangement of the directional growth probabilities may lead to an isotropic structure or any other directional formations. For two-dimensional cases, each grid cell has eight growing directions to its neighbors, as seen in Fig. 2. There are four main directions (1,2,3,4) and four diagonal directions (5,6,7,8). To obtain an isotropic structure in such systems, we set both the main directional growth probabilities D_{1-4} and the diagonal directional growth probabilities D_{5-8} into a constant in each respective group, and the both constants in a fixed ratio. It is the relative value not the absolute value of D_i that controls the anisotropy of structure. For instance by designating the probabilities ratio, $D_{1-4} : D_{5-8} = 4$, we get the directional growth probability consistent with the equilibrium density distribution function for isotropic materials [30,31].

2.3. The lattice Boltzmann algorithm

The lattice Boltzmann method (LBM) is intrinsically a mesoscopic approach based on the evolution of statistical distribution of particles on lattices, and has achieved considerable success in solving various PDEs [32–34,18,19]. The most important advantages of the LBM are the easy implementations of interparticle interactions and the complex geometry boundary conditions [20,21,28,29], and in general the conservation laws of mass or/and energy can hold automatically without additional computational efforts [33]. Additional scheme dealing with the multiphase conjugate boundary conditions has been developed very recently using the LBM method as well and has shown high computation efficiency [19].

For the governing equation, Eq. (1), we employ the evolution equation on discrete lattices for each phase as

$$g_\alpha(\mathbf{r} + \mathbf{e}_\alpha \delta_t, t + \delta_t) - g_\alpha(\mathbf{r}, t) = -\frac{1}{\tau^n}[g_\alpha(\mathbf{r}, t) - g_\alpha^{eq}(\mathbf{r}, t)],$$

(9)

The equilibrium distribution of the evolution variable, g_α, for the two-dimensional nine-speed (D2Q9) model is

$$g_\alpha^{eq} = \begin{cases} 0 & \alpha = 0 \\ U/6 & \alpha = 1,2,3,4 \\ U/12 & \alpha = 5,6,7,8 \end{cases}$$

(10)

the microscopic evolution velocity

$$\mathbf{e}_\alpha = \begin{cases} (0,0) & \alpha = 0 \\ (\cos\theta_\alpha, \sin\theta_\alpha)c, & \theta_\alpha = (\alpha - 1)\pi/2 & \alpha = 1,2,3,4 \\ \sqrt{2}(\cos\theta_\alpha, \sin\theta_\alpha)c, & \theta_\alpha = (\alpha - 5)\pi/2 + \pi/4 & \alpha = 5,6,7,8 \end{cases}$$

(11)

and the dimensionless relaxation time
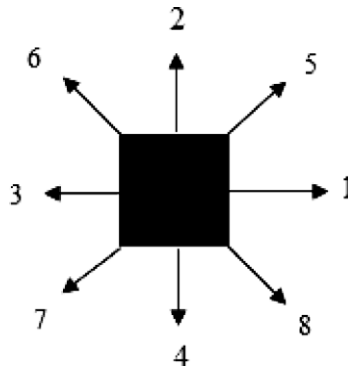
$$\tau^n = \frac{3}{2}\frac{E^n}{c^2 \delta_t} + 0.5$$

(12)

Fig. 2. Eight growth directions of each point for 2D systems.

where the superscript n still represents the nth phase, δ_t the time step, ε_r the relative dielectric constant, and c a *pseudo* sound speed whose value can theoretically take any positive value to insure τ values within $(0.5, 2)$ [18]. The displacement and the force on each lattice are then calculated by

$$U = \sum_\alpha g_\alpha \tag{13}$$

$$F = \left(\sum_\alpha \mathbf{e}_\alpha g_\alpha \right) \frac{\tau^n - 0.5}{\tau^n} \tag{14}$$

For the Dirichlet boundary, we employ the bounce-back rule of the non-equilibrium distribution proposed by Zou and He [35]. After the displacement field is solved, the effective Young's modulus can then be determined based on Eq. (6) as:

$$E_{eff} = \frac{H \cdot \int F \cdot dL}{\Delta U \int dL} \tag{15}$$

3. The existing theoretical models

To validate our numerical method initially, we will compare our results with those of the basic models for materials with simple structures. The simplest theoretical approaches to predict the moduli of two-phase composites are the classical averaging schemes: the Voigt model and the Reuss model [36,37]. The Voigt model assumes the constituents of a composite to be in parallel arrangement subjected to the same strain (isostrain). The effective modulus of the composite is thus given by

$$E_{eff} = E_1 \phi^1 + E_2 (1 - \phi^1) \tag{16}$$

where E_1 and E_2 are the Young's moduli of the phase 1 and phase 2, respectively, and ϕ^1 is the volume fraction of the phase 1.

In the Reuss model, the constituents of the composite are under the same stress (isostress) and the effective modulus is given by

$$E_{eff} = \left[\frac{\phi^1}{E_1} + \frac{(1 - \phi^1)}{E_2} \right]^{-1} \tag{17}$$

Hashin and Shtrikman [1] developed models with assumed macroscopical isotropy and quasi-homogeneity of composites, where the reinforcing particles are uniformly dispersed into the matrix. Depending on whether the stiffness of the matrix material is larger or smaller than that of the reinforcement, the upper and lower bounds of the effective mechanical properties are calculated as:

$$K_c^u = K_p + \frac{1 - \phi}{\frac{1}{K_m - K_p} + \frac{3\phi}{3K_p + 4G_p}} \tag{18}$$

$$K_c^l = K_m + \frac{\phi}{\frac{1}{K_p - K_m} + \frac{3(1 - \phi)}{3K_m + 4G_m}} \tag{19}$$

$$G_c^u = G_p + \frac{1 - \phi}{\frac{1}{G_m - G_p} + \frac{6\phi(K_p + 2G_p)}{5G_p(3K_p + 4G_p)}} \tag{20}$$

$$G_c^l = G_m + \frac{\phi}{\frac{1}{G_p - G_m} + \frac{6(1 - \phi)(K_m + 2G_m)}{5G_m(3K_m + 4G_m)}} \tag{21}$$

where ϕ refers to the volume fraction of the reinforcing particles, K_p, K_m and K_c are the bulk moduli of the particles, matrix and composite, and G_p, G_m and G_c their shear moduli respectively. The superscripts "u" and "l" correspond to the upper and lower bounds, respectively. The upper and lower Hashin–Shtrikman (HS) bounds for the Young's modulus of the composite can then be calculated by [8]:

$$E_{HS} = \frac{9K_c G_c}{3K_c + G_c} \tag{22}$$

where the upper and lower K_c and G_c values are used to determine the respective E_{HS} bounds.

4. Results and discussion

The present methods will first be validated by comparisons with the basic models for composites of simple structures. Then they will be used to deal with multiphase composites with much more complex internal structures and the results will be verified by the experimental data.

4.1. Reproduction of complex multiphase microstructures

Using the present generation method, we have reproduced microstructures for some real multiphase composites based on the experimental information. For instance, Tilbrook et al. [7] provided a series of microstructural images of alumina–epoxy composite samples. Pores are clearly observable in the composites, although the porosity details are not reported. Their results show roughly that the porosity decreases with the alumina volume fraction $\phi^{Al_2O_3}$ when $\phi^{Al_2O_3} \geqslant 50\%$, but increase with $\phi^{Al_2O_3}$ otherwise. Since it is reported that the porosity ε was at most 5% in the Al_2O_3–Epoxy composites, we estimate here a bi-linear relationship between the porosity ε and the alumina volume fraction $\phi^{Al_2O_3}$

$$\varepsilon = \begin{cases} 0.1 \cdot \phi^{Al_2O_3} & (v_f^{Al_2O_3} < 50\%) \\ 0.1 \cdot (1 - \phi^{Al_2O_3}) & (v_f^{Al_2O_3} \geqslant 50\%) \end{cases} \tag{23}$$

Fig. 3 shows six generated random microstructures of the Al_2O_3–Epoxy–Pore composites using our approach on a 200×200 grid system, where the light phase is the alumina, the grey area is the epoxy and the dark spots are the pores. Compared with the microstructure images of the actual composites, see Fig. 1 in Ref. [7], the regenerated ones here have captured the structure details and the stochastic characteristics.
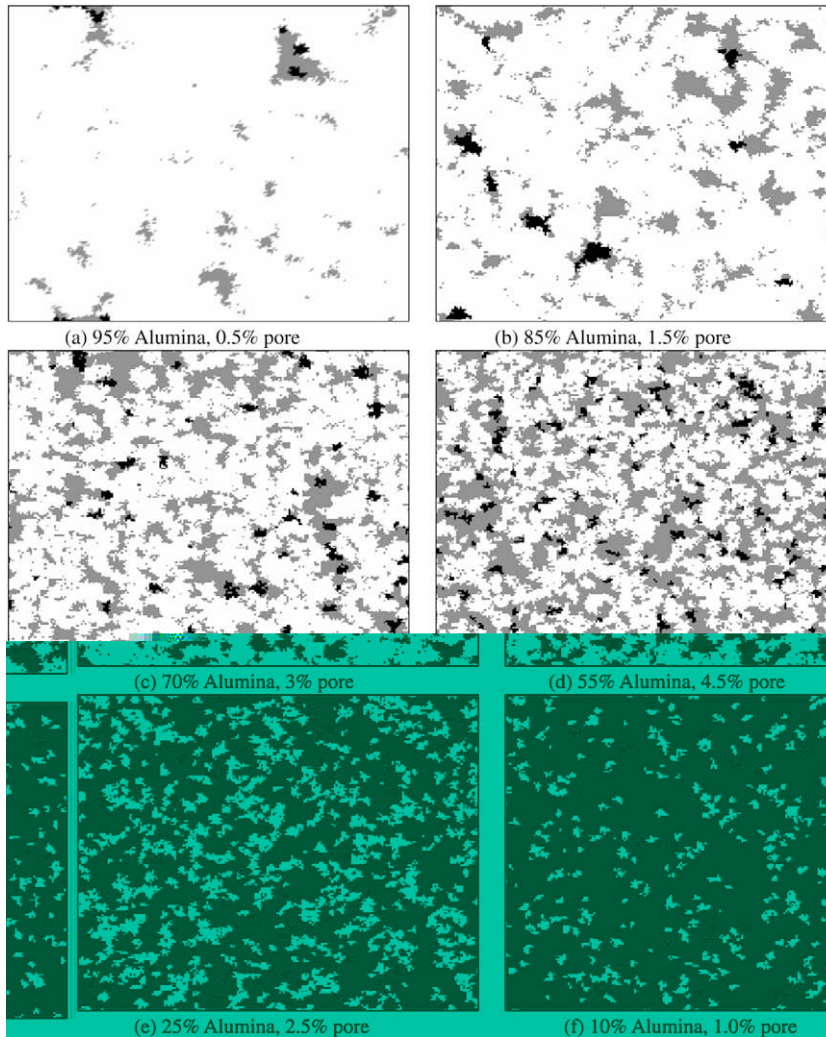

(a) 95% Alumina, 0.5% pore   (b) 85% Alumina, 1.5% pore

(c) 70% Alumina, 3% pore   (d) 55% Alumina, 4.5% pore

(e) 25% Alumina, 2.5% pore   (f) 10% Alumina, 1.0% pore

Fig. 3. Reproduced three-phase microstructures of alumina–epoxy composites by the random generation-growth algorithm. $c_d^{Al_2O_3} = 0.1 \cdot \phi^{Al_2O_3}(1 - \phi^{Al_2O_3})$ and $c_d^{pore} = (1 - \phi^{Al_2O_3}) \cdot c_d^{Al_2O_3}$ for $\phi^{Al_2O_3} \geqslant 50\%$ or $c_d^{pore} = \phi^{Al_2O_3} \cdot c_d^{Al_2O_3}$ for $\phi^{Al_2O_3} < 50\%$.
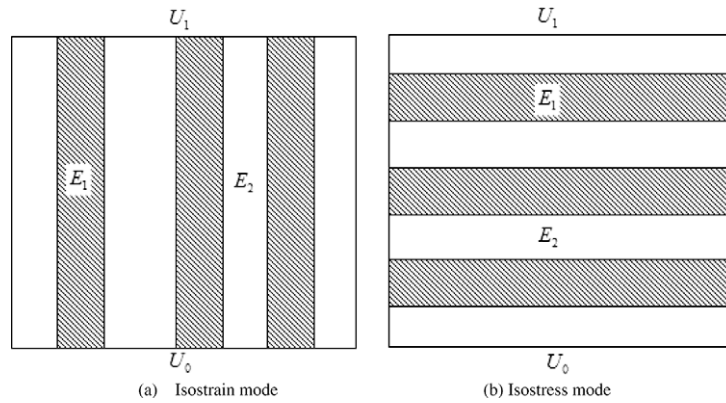
Fig. 4. Two basic structures for validations.

4.2. The benchmarks validations

To validate our methods, we first compare our predicted effective elastic moduli for two simple structures, the parallel and series structures in Fig. 4, with those by the basic models correspondingly. The Voigt model and the Reuss model give exact analytical solutions for these two simple structures in Eqs. (15)–(16), and Fig. 5 compares the predicted effective moduli versus the volume fraction of phase 1, where $E_1 = 1$ GPa and $E_2 = 10$ GPa with our predictions. It is clear that the present methods agree very well with both basic models.

To further demonstrate the robustness of our approach, we allow the modulus ratio $E_1:E_2$ to range from 1:2 to 1:10000 by keeping $E_1 = 1.0$ GPa as a constant. Table 1 lists the calculated effective moduli comparing with the basic solutions for $\phi = 0.5$. Such a large contrast between E_1 and E_2 leads to a long computational time for our algorithms to converge to a steady result, and yet provides a useful test on our model performance. The deviations between the predictions are no greater than 0.006% for the parallel structure and 0.765% for the series structure, showing a good accuracy of our approach.

4.3. The Young's modulus of complex materials

After the validations of our method for simple structures, we apply it to investigating the effective elastic moduli of multiphase composites with complex microstructures. We used the random generation-growth method to reproduce microstructures of the composites as introduced above and then solved the governing equations by the lattice Boltzmann method to obtain the predictions. Then we compare in Fig. 6 our predictions with the measurements as well as the predictions by other theoretical models in [38] for the effective Young's modulus of Al–Al$_2$O$_3$ composites. The properties used in the simulations are listed in Table 2. The present two-phase predictions (solid line with stars) in general seem to have over
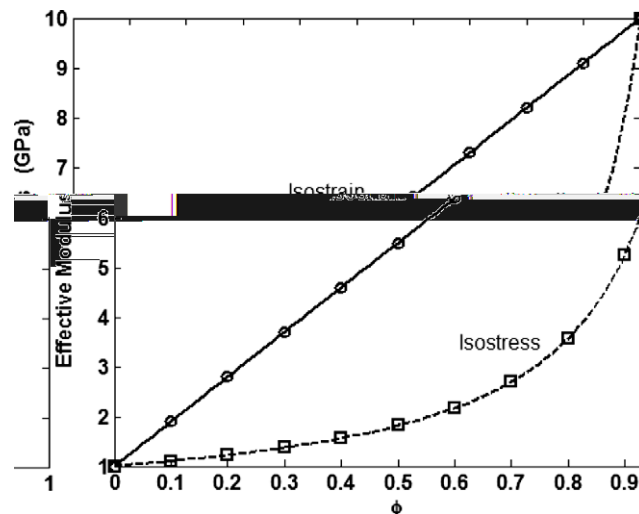

Fig. 5. Comparisons between our predicted effective modulus (symbols) with theoretical models for isostrain and isostress modes (lines) at $E_1 = 1$ GPa and $E_2 = 10$ GPa.

Table 1
Comparisons between predicted results and theoretical solutions where $E_1 = 1.0$ (GPa).

| E_c	Isostrain mode			Isostress mode		
$E_1:E_2$	Voigt model (GPa)	Present predictions (GPa)	Relative deviations (%)	Reuss model (GPa)	Present predictions (GPa)	Relative deviations (%)
1:2	1.500	1.500	0.000	1.333	1.332	0.075
1:10	5.500	5.500	0.000	1.818	1.815	0.165
1:100	50.50	50.50	0.000	1.980	1.976	0.202
1:500	250.5	250.5	0.000	1.996	1.991	0.250
1:1000	500.5	500.5	0.000	1.998	1.993	0.250
1:10000	5000.5	5000.2	0.006	1.9998	2.0151	0.765
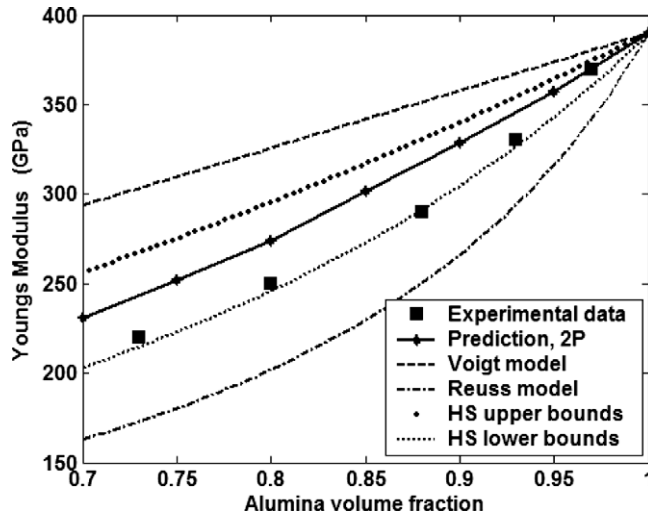
Fig. 6. Comparisons of our two-phase predictions of effective Young's Modulus, as a function of alumina volume fraction, for Al–Al$_2$O$_3$ composites with experimental data [38] and various theoretical modeling results.

estimate composite property when the alumina volume fraction is lower than 0.95. We also noticed that the predicted HS lower bound are sometime even greater than the experimental data, another sign of overestimation. A careful examination of the optical micrographs of the Al—Al$_2$O$_3$ composites in Fig. 1 by Moon et al. [38] shows some visible pores in the samples. We suspect such uncounted material defects may be responsible for the overestimation.

Thus we modify our predictions by including some pores as another phase residing in the composite. We estimated the porosity of such composite roughly at 5% when the alumina volume fraction is no greater than 90%, and at 2.5% otherwise. The elastic modulus of the air is assigned a small value $E_a = 10^{-3}$ GPa in our simulations. Fig. 7 shows our predicted effective Young's moduli for such three-phase composites along with the same experimental data. The agreement becomes much better in general over all the alumina volume fraction range. This indicates that the pores influence on the effect elastic properties of solid composites is not negligible even if the porosity is as small as 2.5%.

Another case we calculated is the alumina–epoxy composite discussed in Section 4.1, and a bi-linear relationship between the porosity and the alumina volume fraction is already given in Eq. (23). We employ such a relationship as in Eq. (23) for our predictions. The properties of alumina and epoxy are listed in Table 2. Fig. 8 shows a good agreement between the predicted effective Young's modulus and the experimental data by Tilbrook et al. [7]. At a high modulus ratio between the two solid components ($E^{Al_2O_3} : E^{epoxy} = 390 : 3.4$), the HS bounds fail to provide acceptable estimations whereas the predictions by the present method again exhibit high agreement with the experimental data. If there were more details on the porosity, the prediction accuracy could be better.

Table 2
Elastic properties of composite-materials.

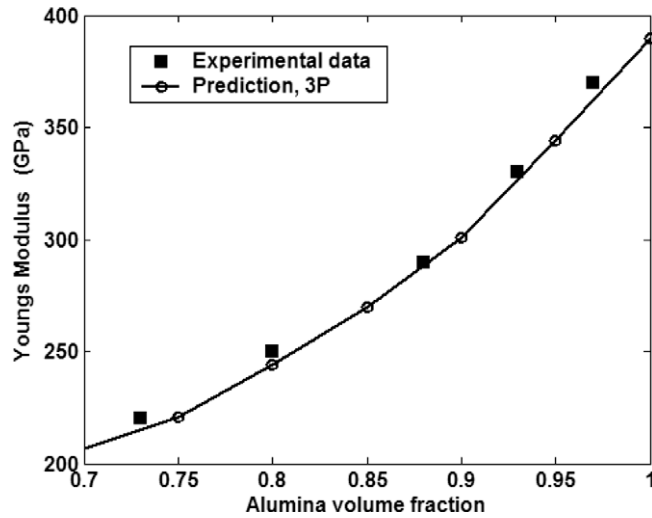| Property	Al$_2$O$_3$	Al	Epoxy
E (GPa)	390	69	3.4
K (GPa)	260	67	3.8
G (GPa)	156	26	1.26

Fig. 7. The three-phase (Al,Al$_2$O$_3$ and air) predictions of effective Young's Modulus, as a function of alumina volume fraction, for Al − Al$_2$O$_3$ composites compared with the experimental data [38]. The air volume fraction, ε, is set at 5% when the alumina volume fraction $\phi_{Al_2O_3} \leqslant 90\%$ and $\varepsilon = 2.5\%$ when $\phi_{Al_2O_3} > 90\%$.
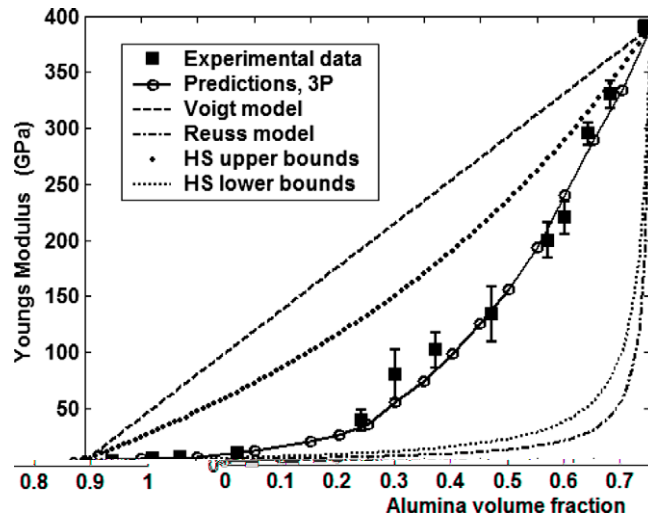

Fig. 8. Comparisons of three-phase (Epoxy, Al$_2$O$_3$, air) predictions of effective Young's Modulus, as a function of alumina volume fraction, for Epoxy–Al$_2$O$_3$ composites with experimental data [7] and various theoretical modeling results. Linear relationships between porosity and volume fraction of alumina are assumed: for $\phi_{Al} \geqslant 50\%$, $\varepsilon = 0.1(1 - \phi_{Al})$; for $\phi_{Al} < 50\%$, $\varepsilon = 0.1\phi_{Al}$.

4.4. The shear modulus and the Poisson's ratio

As mentioned before, when the direction of external force *F* varies from normal to parallel to the top surface, a very similar governing equation as Eq. (1) can be obtained to describe the shear displacement with varying local shear modulus of composite-materials. The modeling process is quite similar to that for effective Young's modulus. Fig. 9 shows the predicted effective shear modulus of alumina–epoxy composites versus the alumina volume fraction for the same three-phase microstructures in Fig. 8. The given shear moduli of Al$_2$O$_3$ and epoxy are listed in Table 2. We assign the shear modulus of pores a tiny value ($G_a = 10^{-5}$ GPa) which actually has little effect on the final predictions. Again with the dispersed pores/voids considered, the predicted effective shear modulus of Al$_2$O$_3$–Epoxy composites agree well with the experimental measurements [7].

After both the Young's modulus and the shear modulus are predicted, by assuming isotropy of the composite at the macro-level, the effective Poisson's ratio is subsequently calculated by [7]

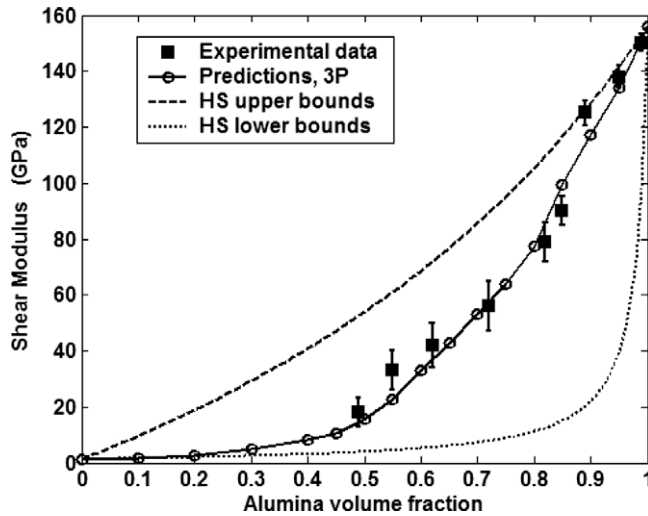$$v = \frac{E}{2G} - 1, \tag{24}$$

Fig. 9. Predicted effective shear Modulus as a function of alumina volume fraction for Al_2O_3–Epoxy–air (three-phase) composites compared with the experimental data [7] and HS bounds.
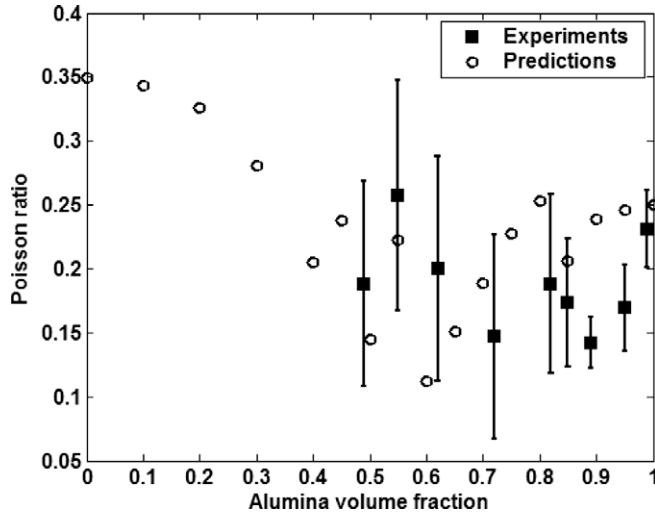

Fig. 10. Comparisons between predicted effective Poisson's ratio as a function of alumina volume fraction for Epoxy–Al_2O_3 composites and the measurements [7].

and the results are compared with the available experimental data in Fig. 10. The theoretical models predict that the Poisson ratio should fall within the region of (0.25,0.35) if the Al_2O_3–Epoxy composite is treated as two-phase only, again an over-estimation of the lower bound. This further confirms that the effects of pores/voids on the effective elastic properties of composites are not negligible.

Note that, in all the cases shown above, the present methods have demonstrated reliable and robust performance for accurate predictions without resorting to any empirical parameters.

5. Conclusions

A new numerical approach for elastic properties prediction of multiphase composites has been developed in this study. A random generation-growth method is proposed for reproducing the complex microstructures of multi-solid composite with dispersed pores/voids inside. A high-efficiency lattice Boltzmann method is then employed to solve the governing equations through multiphase microstructures with complex geometries by varying the local relaxation time corresponding to the local material property. After validated by a few basic models for simple geometries, the present method is used to model the effective elastic properties of several actual composites and the results are compared well with the existing experimental

data. It is demonstrated that despite their tiny amounts, the pores/voids dispersed in composites if ignored likely lead to non-negligible deviations in the predicted effective elastic properties, compared with the experimental measurements. When the pores are taken into account and treated as another separate phase, the predicted Young's modulus, shear modulus and Poisson's ratio agree well with the available experimental data. Although the present governing equations are based on a one-dimensional assumption, they seem to work well for composites of multi-dimensional microstructures. The present method thus provides a robust tool for analysis, design and optimization of multiphase composite-materials, without resorting to empirical parameters

Acknowledgments

References

[1] Z. Hashin, S. Shtrikman, A variational approach to the theory of the elastic behaviours of multiphase materials, J. Mech. Phys. Solids 11 (2) (1963) 127–140.
[2] R.M. Christensen, Mechanics of Composite Materials, Wiley, New York, 1979.
[3] K.A. Snyder, E.J. Garboczi, A.R. Day, The elastic moduli of simple two-dimensional isotropic composites: computer simulation and effective medium theory, J. Appl. Phys. 72 (12) (1992) 5948–5955.
[4] J. Poutet, D. Manzoni, F. HageChehade, C.J. Jacquin, M.J. Bouteca, J.F. Thovert, P.M. Adler, The effective mechanical properties of random porous media, J. Mech. Phys. So1ids 44 (10) (1996) 1587–1620.
[5] P. Rajinder, New models for effective Young's modulus of particulate composites, Composites B 36 (2005) 513–523.
[6] J.P. Watt, G.F. Davies, R.J. O'Cnnell, Elastic properties of composite-materials, Rev. Geophys. 14 (4) (1976) 541–563.
[7] M.T. Tilbrook, R. Moon, M. Hoffman, On the mechanical properties of alumina–epoxy composites with an interpenetrating network structure, Mater. Sci. Eng. A 393 (1–2) (2005) 170–178.
[8] Z. Hashin, Analysis of composite-materials – A survey, J. Appl. Mech. ASME 50 (3) (1983) 481–505.
[9] S. Torquato, Random Heterogeneous Materials: Microstructure and Macroscopic Properties, Springer, New York, 2002.
[10] H.F. Zhang, X.S. Ge, H. Ye, Randomly mixed model for predicting the effective thermal conductivity of moist porous media, J. Phys. D: Appl. Phys. 39 (1) (2006) 220–226.
[11] N. Losic, J.F. Thovert, P.M. Adler, Reconstruction of Porous Media with Multiple Solid Phases, J. Colloid Interf. Sci. 186 (1997) 420–433.
[12] D.S. Li, G. Saheli, M. Khaleel, H. Garmestani, Quantitative prediction of effective conductivity in anisotropic heterogeneous media using two-point correlation functions, Comput. Mater. Sci. 38 (1) (2006) 45–50.
[13] P. Meakin, Fractals, Scaling and Growth Far from Equilibrium, Cambridge University Press, 1998.
[14] M. Wang, J.K. Wang, N. Pan, S.Y. Chen, Mesoscopic predictions of the effective thermal conductivity of microscale random porous media, Phys. Rev. E 75 (2007) 036702.
[15] M. Wang, J.K. Wang, N. Pan, S. Chen, J. He, Three-dimensional effect on the effective thermal conductivity of porous media, J. Phys. D: Appl. Phys. 40 (2007) 260–265.
[16] N. Srikanth, C.V. Lim, M. Gupta, The modeling and determination of dynamic elastic modulus of magnesium based metal matrix composites, J. Mater. Sci. 35 (2000) 4661–4666.
[17] D.P. Mondal, N. Ramakrishnan, S. Das, FEM modeling of the interface and its effect on the elasto-plastic behavior of metal matrix composites, Mater. Sci. Eng. A 433 (1–2) (2006) 286–290.
[18] J.K. Wang, M. Wang, Z.X. Li, Lattice Poisson–Boltzmann simulations of electro-osmotic flows in microchannels, J. Colloid Interf. Sci. 296 (2) (2006) 729–736.
[19] J.K. Wang, M. Wang, Z.X. Li, A lattice Boltzmann algorithm for fluid–solid conjugate heat transfer, Int. J. Thermal Sci. 46 (3) (2007) 228–234.
[20] Q.J. Kang, D.X. Zhang, S.Y. Chen, Unified lattice Boltzmann method for flow in multiscale porous media, Phys. Rev. E 66 (5) (2002) 056307.
[21] Q.J. Kang, D.X. Zhang, S.Y. Chen, Simulation of dissolution and precipitation in porous media, J. Geophys. Res. 108 (2003) 2505.
[22] E.K. Muhammed, H.A. Ahmet, M. Eyad, Laboratory validation of lattice Boltzmann method for modeling pore-scale flow in granular materials, Comput. Geotech. 33 (8) (2006) 381–395.
[23] M. Wang, J.K. Wang, S. Chen, N. Pan, Electrokinetic pumping effects of charged porous media in microchannels using the lattice Poisson–Boltzmann method, J. Colloid Interf. Sci. 304 (1) (2006) 246–253.
[24] M. Wang, S. Chen, Electroosmosis in homogeneously charged micro- and nanoscale random porous media, J. Colloid Interf. Sci. 314 (1) (2007) 264–273.
[25] C.R. Wylie, L.C. Barrett, Advanced Engineering Mathematics, McGraw-Hill Book Company, New York, 1982.
[26] E.J. Garboczi, A.R. Day, An Algorithm for computing the effective linear elastic properties of heterogeneous materials: three-dimensional results for composites with equal phase Poisson ratios, J. Mech. Phys. So1ids 43 (9) (1995) 1349–1362.
[27] S. Meille, E.J. Garboczi, Linear elastic properties of 2D and 3D models of porous materials made from elongated objects, Modell. Simul. Mater. Sci. Eng. 9 (2001) 371–390.
[28] M. Wang, F.K. Meng, N. Pan, Transport properties of functionally graded materials, J. Appl. Phys. 102 (2007) 033514.
[29] M. Wang, N. Pan, Numerical analyses of the effective dielectric constant of multiphase microporous media, J. Appl. Phys. 101 (2007) 114102.
[30] X.Y. He, L.S. Luo, A priori derivation of the lattice Boltzmann equation, Phys. Rev. E 55 (1997) 6333–6336.
[31] T. Abe, Derivation of the lattice Boltzmann method by means of the discrete ordinate method for the Boltzmann equation, J. Comput. Phys. 131 (1997) 241–246.
[32] S.Y. Chen, G.D. Doolen, Lattice Boltzmann method for fluid flows, Annu. Rev. Fluid Mech. 30 (1998) 329–364.
[33] S. Succi, The Lattice Boltzmann Equation for Fluid Dynamics and Beyond, Oxford Science Press, London, 2001.
[34] D. Raabe, Overview of the lattice Boltzmann method for nano- and microscale flow dynamics in materials science and engineering, Modell. Simul. Mater. Sci. Eng. 12 (2004) R13–R46.
[35] Q.S. Zou, X.Y. He, On pressure and velocity boundary conditions for the lattice Boltzmann BGK model, Phys. Fluids 9 (6) (1997) 1591–1598.
[36] W. Kreher, W. Pompe, Internal Stresses in Heterogeneous Solids, Akademie-Verlag, Berlin, 1989.
[37] C.P. Wong, R.S. Bollampally, Thermal conductivity, elastic modulus, and coefficient of thermal expansion of polymer composites filled with ceramic particles for electronic packaging, J. Appl. Polymer Sci. 74 (14) (1999) 3396–3403.
[38] R.J. Moon, M. Tilbrook, M. Hoffman, A. Neubrand, Al–Al$_2$O$_3$ composites with interpenetrating network structures: composite modulus estimation, J. Am. Ceram. Soc. 88 (3) (2005) 666–674.